Does Covalency Decrease with Coordination Number?

Alexey O. Shorikov,[1,2,3] Dmitry M. Korotin,[1,2] Vladimir I. Anisimov,[1,2,3] and Artem R. Oganov[2]
[1)]*M.N. Mikheev Institute of Metal Physics of Ural Branch of the Russian Academy of Sciences, 18 S. Kovalevskaya St., Yekaterinburg, 620108, Russia*
[2)]*Skolkovo Institute of Science and Technology, 30 Bolshoy Boulevard, bld. 1, Moscow, 121205, Russia*
[3)]*Department of Theoretical Physics and Applied Mathematics, Ural Federal University, 19 Mira Str., Yekaterinburg, 620002, Russia*

(*Electronic mail: A.Oganov@skoltech.ru)

(*Electronic mail: alexey.shorikov@gmail.com)

(Dated: 4 August 2025)

It is traditionally believed that the degree of covalency of chemical bonds decreases with increasing coordination number, while the degree of ionicity increases. Using Bader charge analysis and our novel definition of atomic charges based on Wannier functions, we demonstrate that this expectation does not hold for zinc oxide (ZnO) and carbon dioxide (CO_2). The low-pressure wurtzite phase of ZnO (with fourfold coordination of Zn and O) and the high-pressure rocksalt phase (with sixfold coordination) exhibit nearly identical degrees of ionicity. For CO_2, covalency slightly increases in the high-pressure β-cristobalite phase (where the carbon atom is fourfold coordinated) compared to its low-pressure molecular cubic phase (with it is twofold coordinated). Thus, contrary to common belief, the degree of covalency of chemical bonds is governed primarily by the chemical nature of the atoms and their bonding environment, rather than by the coordination number alone.

I. INTRODUCTION

The nature of chemical bonding in solid-state materials remains a central topic in condensed matter physics and materials science. Among all bonding types, covalent bonding is uniquely directional, making the degree of covalency strongly correlated with mechanical properties such as hardness[1] and shear modulus. Ionicity, quantified through atomic charges, directly influences dielectric constants, longitudinal-optical–transverse-optical (LO–TO) splitting, dipole moments, infrared spectra, and numerous other properties. A widely accepted paradigm holds that the degree of covalency decreases with increasing coordination number, while the ionicity correspondingly increases. This view is intuitively justified by the non-directional nature of ionic bonds, which favor high coordination and close-packed structures. In contrast, the classical picture of covalent bonding, rooted in valence bond theory, assumes predominantly two-center bonds, each involving at least one full electron pair (i.e., bond order of one), thereby naturally limiting the coordination number to about four. This simplified model is often used to rationalize trends in electronic structure, bonding character, and macroscopic behavior.

In the present study, we re-examine this conventional assumption by introducing a novel definition of atomic charges based on the analysis of Wannier functions. Using this formalism, we investigate ZnO and CO_2 and show that the degree of ionicity is governed primarily by the intrinsic electronic properties of the constituent atoms and the stoichiometry of the compound, rather than by the coordination number. Our results are supported by Bader charge analysis, which offers a first-principles partitioning of charge density into atomic contributions via integration over zero-flux surfaces, yielding a natural estimate of ionic charges. The Wannier function approach, in contrast, provides a complementary perspective by constructing localized orbitals through a unitary transformation of Bloch states. This allows the electronic structure obtained from density functional theory (DFT) to be expressed in terms of Hamiltonian and occupancy matrices, offering a chemically intuitive framework for bonding analysis. The combination of these two partitioning schemes—one based on the wavefunction and the other on total charge density—enables a more comprehensive understanding of bonding, capturing subtle features of electronic structure and charge distribution often missed in traditional models.

The contrasting bonding properties of ZnO, a wide-bandgap semiconductor, and CO_2, a prototypical molecular solid, offer a compelling basis for comparative analysis. For both compounds, our findings emphasize that the degree of ionicity is determined not so much by the coordination number, but rather by the electronic properties of the constituent atoms and the chemical character of their immediate environment. We offer a rationale for this behavior based on detailed charge and bonding analysis. This investigation contributes to a deeper understanding of charge distribution in complex materials and offers new insight into the nature of chemical bonding.

II. METHODOLOGY

To determine the contributions of ionicity and covalency to the chemical bonds in ZnO, the Wannier function approach was employed. This computational scheme has been successfully applied to investigate chemical bond properties in a series of compounds[2,3]. The band structure calculations were carried out using the GGA (generalized gradient approximation)[4] as implemented in the Quantum Espresso package[5]. All crystal structures were fully optimized prior to further analy-

sis. An effective Hamiltonian $H_{\rm DFT}$ was constructed using the basis of atomic-centered Wannier functions as described in Ref.[6].

Consider a binary compound AB. The chemical bonding energy, $E_{\rm bond}$, is defined as the difference between the total energy of the compound per formula unit at its equilibrium volume V_0 and the sum of the energies of free atoms A and B at infinite separation:

$$E^0_{\rm bond} = E^0_{\rm AB} - (E^\infty_{\rm A} + E^\infty_{\rm B}). \quad (1)$$

From the density functional theory (DFT) solution, we obtain a set of electronic eigenvalues and eigenfunctions, $\varepsilon^\alpha_{\vec{k}}$, $|\psi^\alpha_{\vec{k}}\rangle$, respectively. The electron Hamiltonian is expressed as:

$$\hat{H} = \sum_{\vec{k}\alpha} |\psi^\alpha_{\vec{k}}\rangle \varepsilon^\alpha_{\vec{k}} \langle\psi^\alpha_{\vec{k}}|. \quad (2)$$

The corresponding density matrix operator is:

$$\hat{\rho} = \sum_{\vec{k}\alpha} |\psi^\alpha_{\vec{k}}\rangle n^\alpha_{\vec{k}} \langle\psi^\alpha_{\vec{k}}|, \quad (3)$$

where $n^\alpha_{\vec{k}} = \theta(E_{\rm Fermi} - \varepsilon^\alpha_{\vec{k}})$.

Wannier functions $|W_i\rangle$ are derived through a unitary transformation of the Bloch function set $|\psi^\alpha_{\vec{k}}\rangle$,

$$|W_i\rangle = \sum_{\vec{k}\alpha} |\psi^\alpha_{\vec{k}}\rangle \langle\psi^\alpha_{\vec{k}}|\varphi_i\rangle, \quad (4)$$

where $|\varphi_i\rangle$ are trial atomic wave functions. The resulting Wannier functions $|W_i\rangle$ retain the symmetry of atomic orbitals..

A basis set $|W_i\rangle$ defined by Eq. 4 is then orthonormalized. Wannier functions can be regarded as "natural" atomic orbitals for electrons in a crystal, with index i spanning atomic quantum numbers nl (1s, 2s, 2p, etc.). While Wannier functions are not uniquely defined, the projection procedure in Eq. 4 resolves this ambiguity, yielding functions most similar to atomic orbitals.

Wannier functions $|W_i\rangle$ from Eq. 4 are in real space representation. Sometimes, it is useful to define the reciprocal space representation $|W_{i\vec{k}}\rangle$ for them,

$$|W_{i\vec{k}}\rangle = \sum_{\vec{T}} \exp(-i\vec{k}\cdot\vec{T})|W_i\rangle, \quad (5)$$

where $\vec{T}$ is the translation vector, i is an atomic number in the crystal unit cell, and α is a band number.

The Hamiltonian and density matrix in the Wannier function basis are redefined as:

$$\hat{H} = \sum_{\vec{k}}\sum_{ij} |W_i\rangle \hat{H}^{\vec{k}}_{ij} \langle W_j|,$$
$$\hat{\rho} = \sum_{\vec{k}}\sum_{ij} |W_i\rangle \hat{Q}^{\vec{k}}_{ij} \langle W_j|. \quad (6)$$

The electronic energy E is then:

$$E = {\rm Tr}(\hat{\rho}\hat{H}) = \sum_{\vec{k}}\sum_{ij} Q^{\vec{k}}_{ij} H^{\vec{k}}_{ji} =$$
$$= \sum_{\vec{k}}\sum_{i} Q^{\vec{k}}_{ii} H^{\vec{k}}_{ii} + \sum_{\vec{k}}\sum_{ij,i\neq j} Q^{\vec{k}}_{ij} H^{\vec{k}}_{ji}. \quad (7)$$

To decompose E in Eq. 7 into covalent and ionic contributions, the interatomic term $\sum_{\vec{k}}\sum_{ij,i\neq j} Q^{\vec{k}}_{ij} H^{\vec{k}}_{ji} = \sum_{ij,i\neq j} E_{ij}$ represents covalent energy, while the diagonal term $\sum_i E_{ii} = \sum_{\vec{k}}\sum_i Q^{\vec{k}}_{ii} H^{\vec{k}}_{ii}$ includes both covalent and ionic contributions. By defining average energies $H_i = \sum_{\vec{k}} H^{\vec{k}}_{ii}$ and average occupancy $Q_i = \sum_{\vec{k}} Q^{\vec{k}}_{ii}$ for atom i, the ionic and covalent components are separated as:

$$E^{\rm ion} = \sum_i E^{\rm ion}_i = \sum_i Q_i H_i, \quad (8)$$
$$E^{\rm cov} = \sum_{ij,i\neq j} E_{ij} + \sum_i E_{ii} - \sum_i Q_i H_i.$$

In a general case with orbital indexes $L = (l,m)$, Eq. 7 is:

$$E = {\rm Tr}(\hat{\rho}\hat{H}) = \sum_{\vec{k}}\sum_{iL,jL'} Q^{\vec{k}}_{iL,jL'} H^{\vec{k}}_{jL',iL} \quad (9)$$
$$= \sum_{\vec{k}}\sum_{iL,iL'} Q^{\vec{k}}_{iL,iL'} H^{\vec{k}}_{iL',iL} + \sum_{\vec{k}}\sum_{iL,jL'} Q^{\vec{k}}_{iL,jL'} H^{\vec{k}}_{jL',iL}.$$

For the binary compound AB, the chemical bonding energy [Eq. 1] is

$$E_{\rm bond} = E_{\rm AB} - (E^\infty_{\rm A} + E^\infty_{\rm B})$$
$$= E^{\rm cov} + E^{\rm ion} - (H^\infty_{\rm A} Q^\infty_{\rm A} + H^\infty_{\rm B} Q^\infty_{\rm B}). \quad (10)$$

The following approximation could be useful:

$$H^\infty_A = H_A = \sum_{\vec{k}} H_{AA},$$
$$H^\infty_B = H_B = \sum_{\vec{k}} H_{BB}. \quad (11)$$

Then, from Eqs. 9 and 10,

$$E_{\rm bond} = E^{\rm cov} + E^{\rm ion} - (H_A Q^\infty_A + H_B Q^\infty_B),$$
$$E^{\rm ion} = E^{\rm ion}_A + E^{\rm ion}_B = Q_A H_A + Q_B H_B, \quad (12)$$
$$E^{\rm cov} = 2E_{AB} + E_{AA} - Q_A H_A + E_{BB} - Q_B H_B.$$

Hence, the bonding energy separation is

$$E_{\rm bond} = E^{\rm cov}_{\rm bond} + E^{\rm ion}_{\rm bond},$$
$$E^{\rm ion}_{\rm bond} = E^{\rm ion}_A + E^{\rm ion}_B - (H_A Q^\infty_A + H_B Q^\infty_B)$$
$$= (Q_A - Q^\infty_A) H_A + (Q_B - Q^\infty_B) H_B, \quad (13)$$
$$E^{\rm cov}_{\rm bond} = E^{\rm cov} = 2E_{AB} + E_{AA} - Q_A H_A + E_{BB} - Q_B H_B.$$

The covalent contribution to the bonding energy $E^{\rm cov}_{\rm bond}$ in Eqs. 13 and 14 contains, by definition (see Eq. 9), only off-diagonal terms of Hamiltonian and density matrices in the Wannier basis having atomic orbital symmetry (Eq. 6). Hence, it directly corresponds to the usual chemical understanding of covalent bond between atomic orbitals. However, the ionic part is defined by contribution from diagonal terms of those matrices minus $H_A Q^\infty_A + H_B Q^\infty_B$ term. Hence, it contains not only an ion–ion interaction in crystal but also the energy of transferring the electrons to/from the neutral atoms forming charged ions.

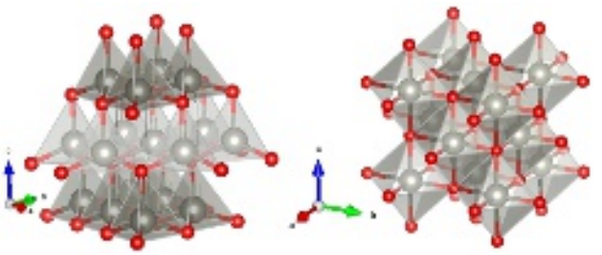

FIG. 1. Crystal structures of ZnO in the wurtzite (left panel) and rocksalt (right panel) phases. Gray and red spheres represent Zn and O atoms, respectively.

Clearly, completely ionic bonding with full charge transfer is impossible from the viewpoint of quantum mechanics, and some degree of covalency is present even in such textbook examples of ionic bonding as NaCl. One of the main advantages of the Wannier function–based analysis is its ability to quantitatively disentangle the ionic and covalent contributions to the total bonding energy.

III. IONICITY AND COVALENCY IN ZnO PHASES

Zinc oxide exists in two primary structural phases: the wurtzite phase, characterized by tetrahedral coordination of Zn and O atoms, and the rocksalt phase, featuring octahedral coordination. At ambient conditions, the equilibrium phase of ZnO is the wurtzite structure. However, under moderate pressure (approximately 9 GPa), ZnO undergoes a phase transition to the cubic rocksalt structure (see Fig. 1). This behavior is consistent with trends observed in other II–VI semiconductors, where structural transitions toward denser configurations, such as the NaCl-type lattice, are favored under pressure due to enhanced interactions beyond the first coordination shell—particularly long-range Coulomb interactions.

This conventional understanding suggests that the wurtzite phase is predominantly covalent, whereas the cubic phase is predominantly ionic. The transition from the wurtzite to the rocksalt phase has been extensively investigated in previous theoretical studies using first-principles calculations[7–13].

To validate our results based on Wannier function analysis, we additionally performed a Bader charge analysis. This method provides a first-principles partitioning of the electronic charge density into "atomic" contributions by integrating over volumes bounded by zero-flux surfaces in the gradient of the charge density. These regions represent the most natural definition of atomic charges in real space. Within each Bader volume, the charge density typically decreases from the nucleus outward, reaching a minimum at the boundary surface, and then increases again into the neighboring atomic regions.

In the Wannier formalism, ionic charges are defined through the occupancy of the corresponding Wannier functions W_i, which are obtained by projecting atomic orbitals ϕ_i onto Bloch functions (see Eq. (4)). Each Wannier function includes only a fraction x_i of the original atomic orbital ϕ_i, while the remaining electronic weight is distributed over neighboring atoms. Therefore, to recover the charge associated with the atomic orbital ϕ_i, the occupancy of W_i must be renormalized by the factor x_i.

Applying this renormalization yields ionic charges of $Z_{\mathrm{Zn}} = +1.11$ for ZnO in the cubic phase and $Z_{\mathrm{Zn}} = +1.10$ in the wurtzite phase. These values are in very good agreement with those obtained from Bader charge analysis.

The total DFT energy of the rocksalt phase of ZnO is 0.248 eV per formula unit (or 0.12 eV per atom) higher than that of the wurtzite phase. This energy difference confirms that the wurtzite structure, characterized by tetrahedral coordination, is indeed the ground-state phase, whereas the cubic rocksalt structure is metastable under ambient conditions.

The full results of the Wannier function analysis are summarized in Table I.

TABLE I. Comparison of the rocksalt and wurtzite phases of ZnO. The total pairwise covalent bonding energy, $\sum E_{\text{pair-bond}}$, is calculated as $E_{\text{pair-bond}}$ multiplied by 6 for the cubic phase and by 4 for the wurtzite phase. The covalent energy fraction (CEF) is defined as $E^{\text{cov}}/E_{\text{bond}}$.

	Rocksalt Phase	Wurtzite Phase
Z_{O}	-0.94	-0.97
Coordination	6	4
E^{cov}, eV/f.u.	-23.73	-22.53
E^{ion}, eV/f.u.	-2.60	-3.65
E_{bond}, eV/f.u.	-26.33	-26.18
$\sum E_{\text{pair-bond}}$, eV/f.u.	-20.00	-20.77
CEF	90%	86%

Here, $E_{\text{pair-bond}}$ denotes the covalent energy of a single metal–oxygen bond. Notably, in the tetrahedral wurtzite phase—characterized by a shorter metal–oxygen distance compared to the cubic rocksalt phase—each Zn–O pair exhibits a stronger covalent interaction: $E_{\text{pair-bond}} = -3.2$ eV in the rocksalt phase and $E_{\text{pair-bond}} = -5.2$ eV in the wurtzite phase.

In the rocksalt structure, each zinc atom is octahedrally coordinated, forming six Zn–O bonds, whereas in the wurtzite phase, it forms only four bonds. Consequently, the total covalent energy summed over nearest neighbors is higher in the wurtzite phase. However, when contributions from more distant neighbors are included, the total covalent energy in the rocksalt phase becomes slightly larger. This can be attributed to the denser packing in the rocksalt structure, which enhances orbital overlap beyond the first coordination shell.

Given that Wannier functions are spatially more extended than atomic orbitals, they tend to overestimate hybridization with distant atoms relative to classical valence bond models based on atomic orbitals. Nevertheless, the total covalent energy is comparable in both phases, with the wurtzite phase gaining a slight energetic advantage due to a marginally higher ionic contribution, as evidenced by the slightly larger ionic charges.

This finding contradicts the conventional expectation that ionicity should increase in the rocksalt phase due to its higher

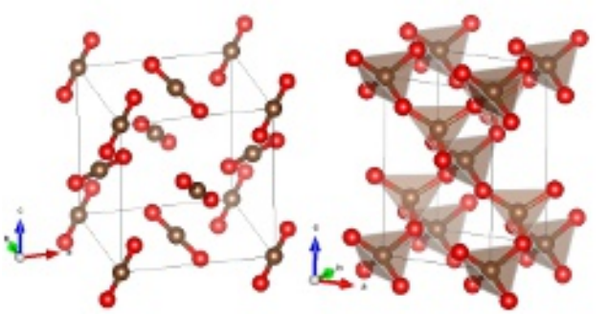

FIG. 2. Crystal structures of CO_2 in the molecular cubic phase (left panel) and the polymeric β-cristobalite phase (right panel). Brown and red spheres represent carbon and oxygen atoms, respectively.

coordination number.

The Bader charge analysis supports this conclusion. For the rocksalt phase, the computed charges are $Z_{\mathrm{Zn}} = +1.20$ and $Z_{\mathrm{O}} = -1.20$, while for the wurtzite phase they are $Z_{\mathrm{Zn}} = +1.19$ and $Z_{\mathrm{O}} = -1.19$. Thus, the variation in ionicity across the phase transition is negligible and within the margin of computational accuracy. The Wannier function approach yields consistent results: $Z_{\mathrm{Zn}} = +0.92$ and $Z_{\mathrm{O}} = -0.92$ for the rocksalt phase, and $Z_{\mathrm{Zn}} = +0.97$ and $Z_{\mathrm{O}} = -0.97$ for the wurtzite phase.

IV. IONICITY AND COVALENCY IN CO_2 PHASES

At ambient pressure and low temperatures, solid CO_2 (commonly known as "dry ice") adopts a prototypical molecular crystal structure. In this phase, the cubic $Pa\bar{3}$ structure consists of well-separated, linear CO_2 molecules[14]. Upon increasing pressure, CO_2 undergoes a sequence of structural phase transitions: first into the *Cmna* phase at approximately 10 GPa, then into a pseudotetragonal phase with $P4_2/mnm$ symmetry around 20 GPa, and finally into the β-cristobalite phase (space group $I\bar{4}2d$) above 35 GPa and 1800 K[15–19].

As is typical for pressure-induced transitions, CO_2 exhibits an increase in coordination number with increasing pressure. In the low-pressure molecular $Pa\bar{3}$ phase, each carbon atom is linearly coordinated with two oxygen atoms (twofold coordination). In contrast, in the high-pressure polymeric β-cristobalite phase, each carbon atom adopts a tetrahedral environment (fourfold coordination), as illustrated in Fig. 2. Our objective is to determine how the atomic charges evolve during this structural phase transition.

From the Bader charge analysis of the molecular cubic phase of CO_2, we obtained $Z_{\mathrm{C}} = +2.14$ and $Z_{\mathrm{O}} = -1.06$, whereas in the β-cristobalite phase the corresponding values are $Z_{\mathrm{C}} = +1.96$ and $Z_{\mathrm{O}} = -0.98$. These results indicate a slight decrease in ionicity and a corresponding increase in covalency upon the phase transition, in contrast to the conventional expectation that ionicity should increase with coordination number. The Wannier function analysis supports this trend, yielding $Z_{\mathrm{C}} = +1.85$ and $Z_{\mathrm{O}} = -0.93$ for the molecular cubic phase, and $Z_{\mathrm{C}} = +1.63$ and $Z_{\mathrm{O}} = -0.81$ for the β-cristobalite phase.

The results of the Wannier function calculations are summarized in Table II.

TABLE II. Comparison between the molecular cubic and polymeric β-cristobalite phases of CO_2. The total covalent bonding energy $\sum E_{\text{pair-bond}}$ is obtained by multiplying the single bond energy $E_{\text{pair-bond}}$ by 2 for the molecular cubic phase and by 4 for the β-cristobalite phase, corresponding to the number of C–O bonds per carbon atom in each structure. The covalent energy fraction (CEF) is defined as $E^{\text{cov}}/E_{\text{bond}}$.

	β-cristobalite Phase	Molecular cubic Phase
Z_{O}	-0.81	-0.93
Coordination	4	2
E^{cov}, eV/f.u.	-61.23	-41.90
E^{ion}, eV/f.u.	-10.03	-14.20
E_{bond}, eV/f.u.	-71.26	-56.11
$\sum E_{\text{pair-bond}}$, eV/f.u.	-57.91	-34.67
CEF	86%	74%

Here, $E_{\text{pair-bond}}$ denotes the covalent energy associated with a single C–O bond. Notably, in the β-cristobalite phase, the C–O bond length increases to 1.402 Å compared to 1.171 Å in the molecular cubic $Pa\bar{3}$ phase. Despite this increase in bond length, the pairwise bond energy becomes significantly more negative: $E_{\text{pair-bond}} = -17.73\,\text{eV}$ in the molecular cubic phase and $-14.46\,\text{eV}$ in the β-cristobalite phase. Moreover, in the β-cristobalite structure, each carbon atom forms four bonds, as opposed to two in the molecular phase, leading to a substantial increase in the total covalent energy. Simultaneously, the ionic contribution decreases due to a reduction in the effective atomic charges, as evidenced by both Wannier function and Bader charge analyses.

Due to the substantial spatial extension of the Wannier functions and their pronounced delocalization onto neighboring atoms, the same formalism can be employed to estimate covalent bonding energies not only for atoms in the first coordination shell but also for those in the second and third coordination spheres. In the molecular cubic phase of CO_2, we find that the covalent bonding energy $E_{\text{pair-bond}}$ between oxygen atoms within the same O–C–O molecule is approximately -1.60 eV. In contrast, the interaction between oxygen atoms from adjacent CO_2 molecules is significantly weaker, ranging from -0.42 eV to -0.74 eV, depending on the mutual orientation of the molecules.

Furthermore, the covalent bonding energy associated with oxygen atoms in the third coordination sphere is nearly uniform, with a typical magnitude of about -0.68 eV. This uniformity suggests that, at such distances, the interaction strength is governed primarily by the spatial extent and symmetry of the overlapping Wannier functions rather than by specific molecular arrangements. Although these long-range contributions are weaker than nearest-neighbor interactions, they still make a non-negligible contribution to the overall cohesive energy and should be considered in accurate energy decomposition analyses.

It is important to note that the calculated bonding energy is

not equivalent to the atomization energy, as the one-electron energies derived from Wannier functions do not account for the significant repulsive interactions arising from the overlap of neighboring electron clouds. These repulsive contributions are instead captured within the total DFT energy E_{tot} via integration over the electron density. As a result, the magnitude of the bonding energy components for CO_2 is greater than that for ZnO and shows a reasonable correlation with the interatomic distances between oxygen and carbon or zinc atoms.

The total DFT energy of the CO_2 β-cristobalite phase is 1.388 eV per formula unit higher than that of the molecular cubic phase. This energy difference confirms that the molecular cubic phase is the thermodynamically stable ground state, in agreement with experimental observations.

V. IONICITY AND COVALENCY IN NaCl

NaCl is a textbook example of an ionic compound. The crystal structure of its ambient-pressure phase ("rocksalt structure") is characterized by sixfold coordination of Na and Cl, while in the high-pressure CsCl-type phase coordination is eightfold[20,21]. Our results are shown in Table III.

TABLE III. Comparison between the rocksalt and the CsCl-type structures of NaCl. The total covalent bonding energy $\sum E_{\text{pair-bond}}$ is obtained by multiplying the single bond energy $E_{\text{pair-bond}}$ by 6 for the rocksalt and by 8 for the CsCl-type phase, corresponding to the number of Na–Cl bonds per sodium atom in each structure. The covalent energy fraction (CEF) is defined as $E^{\text{cov}}/E_{\text{bond}}$.

	CsCl-type structure	NaCl-type structure
Z_{Cl}	-0.79	-0.80
Coordination	8	6
E^{cov}, eV/f.u.	-3.16	-3.18
E^{ion}, eV/f.u.	-5.31	-5.88
E_{bond}, eV/f.u.	-8.47	-9.05
$\sum E_{\text{pair-bond}}$, eV/f.u.	-3.06	-3.00
CEF	37%	35%

Here, $E_{\text{pair-bond}}$ denotes the covalent energy associated with a single Na–Cl bond. In contrast to the CO_2 case, in NaCl $E_{\text{pair-bond}}$ varies with the bond length: in the NaCl-type structure, the Na–Cl bond length is 2.851 Å and the pairwise bond energy is $E_{\text{pair-bond}} = -0.50\,\text{eV}$, whereas in the CsCl-type structure the bond length increases to 3.038 Å and the pairwise bond energy becomes significantly less negative, $-0.38\,\text{eV}$. Similar to ZnO and CO_2, the degree of covalency slightly increases with increasing coordination number.

VI. DISCUSSION

The commonly held expectation that lower coordination numbers correspond to greater covalency and reduced ionicity is based on several assumptions:

1. The assumption that covalent bonding is predominantly characterized by two-center, two-electron bonds. This view implies that coordination numbers exceeding four are unfavorable for covalent bonding. However, this perspective is overly simplistic, as demonstrated by numerous examples in boron chemistry and boranes, where multicenter bonding plays a key role.

2. The notion that covalent interactions are directional while ionic interactions are non-directional, leading to the belief that low coordination numbers are inherently associated with covalency, whereas high coordination numbers favor ionicity. This reasoning is flawed, as coordination numbers in ionic compounds are primarily determined by the ratio of ionic radii. Low coordination numbers can occur in ionic systems when there is a significant size mismatch between cations and anions. Conversely, high coordination numbers are also possible in covalent systems when multicenter bonding is taken into account.

3. Based on the correct notion that covalent bonding is short-ranged, whereas ionic bonding is governed by long-range Coulomb interactions, it is tempting to assume that open structures with low coordination numbers are more likely to exhibit covalency, while dense structures are likely to have higher Madelung constants and display greater degree of ionicity. However, there is nothing to preclude the presence of strong covalent bonding in densely packed structures.

On the other hand, if one considers electronegativity as the negative of the electronic chemical potential of an atom, it follows naturally that electrons should transfer from the less electronegative atom to the more electronegative one until their electronegativities become equal[22]. Since both electronegativity and its dependence on atomic charge (determined by the chemical hardness) are intrinsic atomic properties, the atomic charges at which electronegativities equalize should, to a first approximation, be independent of the crystal structure.

There are also arguments supporting a decrease in ionicity with increasing coordination number:

1. In the ionic picture, higher cation charges are associated with smaller cationic radii. Lower coordination numbers, which are often observed for small cations, are thus consistent with higher ionicity.

2. Covalent bonding at low coordination numbers leads to a higher concentration of valence electrons in individual bonds, which can be energetically unfavorable. A partial shift of this charge density toward the more electronegative anion increases ionicity and can enhance the overall stability of the system.

As our results demonstrate, contrary to the conventional expectation, the degree of ionicity does not increase with coordination number. In fact, in the studied cases, it slightly decreases.

VII. CONCLUSIONS

In this study, we employ density functional theory (DFT) to explore the relationship between atomic coordination and the degree of covalency in chemical bonding. Using Wannier function-based charge partitioning, we analyze ZnO and CO_2 across different structural phases and provide a refined understanding of the interplay between covalent and ionic contributions. In ZnO, the wurtzite phase (with fourfold coordination) exhibits slightly higher ionicity, whereas the high-pressure rocksalt phase (sixfold coordination) demonstrates a more pronounced covalent character, with covalent contributions accounting for 92% of the bonding energy, compared to 86% in the low-pressure phase. In CO_2, covalency increases from 74% in the molecular cubic phase to 86% in the β-cristobalite phase under pressure. These results challenge the conventional view that higher coordination necessarily leads to increased ionicity. Instead, our findings indicate that bond character is primarily governed by intrinsic atomic properties—such as electronegativity and chemical hardness—rather than coordination number alone.

ACKNOWLEDGMENTS

The DFT part of the study carried out within the framework of the state assignment of the Ministry of Science and Higher Education of the Russian Federation for the IMP UB RAS. The analysis of chemical bonding was supported by the state assignment of the Russian Science Foundation (Project 19-72-30043).

AUTHOR DECLARATION

Conflict of interest

The authors have no conflicts to disclose.

AUTHOR CONTRIBUTIONS

Alexey O. Shorikov: Formal analysis (equal); Investigation (lead); Writing – review & editing (equal). **Dmitry M. Korotin**: Formal analysis (equal); Software (lead); Writing – review & editing (equal). **Vladimir I. Anisimov**: Conceptualization (equal); Methodology (lead); Supervision (equal); Formal analysis (equal); Writing – review & editing (equal). **Artem R. Oganov**: Funding acquisition (lead); Project administration (lead); Supervision (equal); Conceptualization (equal); Formal analysis (equal); Writing – review & editing (equal).

DATA AVAILABILITY

The data that support the findings of this study are available from the corresponding author upon reasonable request.

[1]Z. Li, H. Qian, J. Wu, B. L. Gu, and W. Duan, "Role of symmetry in the transport properties of graphene nanoribbons under bias," Physical Review Letters **100**, 21–24 (2008), 1005.0115.
[2]V. I. Anisimov, A. R. Oganov, D. M. Korotin, D. Y. Novoselov, A. O. Shorikov, and A. S. Belozerov, "First-principles definition of ionicity and covalency in molecules and solids," The Journal of Chemical Physics **160**, 144113 (2024).
[3]D. Y. Novoselov, D. M. Korotin, M. A. Mazannikova, V. I. Anisimov, and A. R. Oganov, "Towards understanding the driving forces of the formation of multicomponent compounds: The case of complex oxides," The Journal of Chemical Physics **162**, 204106 (2025).
[4]J. P. Perdew, K. Burke, and M. Ernzerhof, "Generalized Gradient Approximation Made Simple." Phys. Rev. Lett. **77**, 3865 (1996).
[5]P. Giannozzi, S. Baroni, N. Bonini, M. Calandra, R. Car, C. Cavazzoni, D. Ceresoli, G. L. Chiarotti, M. Cococcioni, I. Dabo, A. D. Corso, S. de Gironcoli, S. Fabris, G. Fratesi, R. Gebauer, U. Gerstmann, C. Gougoussis, A. Kokalj, M. Lazzeri, L. Martin-Samos, N. Marzari, F. Mauri, R. Mazzarello, S. Paolini, A. Pasquarello, L. Paulatto, C. Sbraccia, S. Scandolo, G. Sclauzero, A. P. Seitsonen, A. Smogunov, P. Umari, R. M. Wentzcovitch, A. Dal Corso, S. de Gironcoli, S. Fabris, G. Fratesi, R. Gebauer, U. Gerstmann, C. Gougoussis, A. Kokalj, M. Lazzeri, L. Martin-Samos, N. Marzari, F. Mauri, R. Mazzarello, S. Paolini, A. Pasquarello, L. Paulatto, C. Sbraccia, S. Scandolo, G. Sclauzero, A. P. Seitsonen, A. Smogunov, P. Umari, and R. M. Wentzcovitch, "QUANTUM ESPRESSO: a modular and open-source software project for quantum simulations of materials," Journal of Physics: Condensed Matter **21**, 395502 (2009).
[6]D. Korotin, A. V. Kozhevnikov, S. L. Skornyakov, I. Leonov, N. Binggeli, V. I. Anisimov, and G. Trimarchi, "Construction and solution of a Wannier-functions based Hamiltonian in the pseudopotential plane-wave framework for strongly correlated materials," The European Physical Journal B **65**, 91–98 (2008).
[7]J. M. Recio, M. A. Blanco, V. Luaña, R. Pandey, L. Gerward, and J. Staun Olsen, "Compressibility of the high-pressure rocksalt phase of ZnO," Physical Review B **58**, 8949–8954 (1998).
[8]H. Karzel, W. Potzel, M. Köfferlein, W. Schiessl, M. Steiner, U. Hiller, G. M. Kalvius, D. W. Mitchell, T. P. Das, P. Blaha, K. Schwarz, and M. P. Pasternak, "Lattice dynamics and hyperfine interactions in ZnO and ZnSe at high external pressures," Physical Review B **53**, 11425–11438 (1996).
[9]F. Decremps, F. Datchi, A. M. Saitta, A. Polian, S. Pascarelli, A. Di Cicco, J. P. Itié, and F. Baudelet, "Local structure of condensed zinc oxide," Physical Review B **68**, 104101 (2003).
[10]R. Ahuja, L. Fast, O. Eriksson, J. M. Wills, and B. Johansson, "Elastic and high pressure properties of ZnO," Journal of Applied Physics **83**, 8065–8067 (1998).
[11]A. Seko, F. Oba, A. Kuwabara, and I. Tanaka, "Pressure-induced phase transition in ZnO and ZnO-MgO pseudobinary sys," Physical Review B **72**, 024107 (2005).
[12]A. Schleife, F. Fuchs, J. Furthmüller, and F. Bechstedt, "First-principles study of ground- and excited-state properties of MgO, ZnO, and CdO polymorphs," Physical Review B **73**, 245212 (2006).
[13]H. Y. Wu, X. L. Cheng, C. H. Hu, and P. Zhou, "The structure and thermodynamic properties of zinc oxide with wurtzite and rocksalt structure under high pressures," Physica B: Condensed Matter **405**, 606–612 (2010).
[14]R. T. Downs and M. S. Somayazulu, "Carbon Dioxide at 1.0 GPa," Acta Crystallographica Section C Crystal Structure Communications **54**, 897–898 (1998).
[15]C. S. Yoo, H. Kohlmann, H. Cynn, M. F. Nicol, V. Iota, and T. LeBihan, "Crystal structure of pseudo-six-fold carbon dioxide phase II at high pressures and temperatures," Physical Review B **65**, 104103 (2002).
[16]F. Datchi, B. Mallick, A. Salamat, and S. Ninet, "Structure of Polymeric Carbon Dioxide," Physical Review Letters **108**, 125701 (2012).
[17]F. Datchi, M. Moog, F. Pietrucci, and A. M. Saitta, "Polymeric phase V of carbon dioxide has not been recovered at ambient pressure and has a

unique structure," Proceedings of the National Academy of Sciences **114**, E656–E657 (2017).
[18]C.-S. Yoo, M. Kim, W. Morgenroth, and P. Liermann, "Transformation and structure of silicatelike CO_2-V ," Physical Review B **87**, 214103 (2013).
[19]X. Yong, H. Liu, M. Wu, Y. Yao, J. S. Tse, R. Dias, and C. S. Yoo, "Crystal structures and dynamical properties of dense CO2," Proceedings of the National Academy of Sciences of the United States of America **113**, 11110–11115 (2016).
[20]W. A. Bassett, T. Takahashi, H.-K. Mao, and J. S. Weaver, "Pressure-Induced Phase Transformation in NaCl," Journal of Applied Physics **39**, 319–325 (1968).
[21]W. Zhang and A. R. Oganov, "Unexpected Stabel Stochiometries of Sodium Chlorides.pdf," Science **342**, 1502–1505 (2013).
[22]W. J. Mortier, S. K. Ghosh, and S. Shankar, "Electronegativity Equalization Method for the Calculation of Atomic Charges in Molecules," Journal of the American Chemical Society **108**, 4315–4320 (1986).